Nonlinear Panel Response from a Turbulent Boundary Layer

R. VAICAITIS,* C. M. JAN,† AND M. SHINOZUKA‡
Columbia University, New York

The vibration of a flexible elastic plate is investigated by a Monte Carlo technique. The response analysis is performed in time domain by numerically simulating the resulting generalized forces. The nonlinear plate deflection and mutual interaction between the plate motion and external and/or internal airflow is included. The fluid perturbations due to the structural motion are described by linear aerodynamic theory. The boundary-layer pressure field is idealized as a homogeneous multidimensional Gaussian random process with mean zero. The plate differential equations of motion and boundary conditions are satisfied in a Galerkin sense by developing a modal solution. Illustrative examples are presented for subsonic and supersonic flow regions using shallow cavity and two plate mode approximations.

Nomenclature

a = plate length
a_∞ = velocity of sound, external flow
a_c = velocity of sound, cavity flow
b = plate width
b_{ij} = modal amplitude
D = $Eh^2/12(1-\nu^2)$, plate stiffness
d = cavity depth
E = modulus of elasticity
$\bar{F}_{mn}$ = random generalized force
$\bar{F}_{mn}{}^e, \bar{F}_{mn}{}^c$ = aerodynamic generalized forces, external and cavity flow, respectively
i = imaginary unit $(-1)^{1/2}$
h = plate thickness
k_1, k_2, k_3 = wave numbers in x_1, x_2, x_3 directions, respectively
k_{1l}, k_{2l}, k_{3l} = lower bound wave numbers
k_{1u}, k_{2u}, k_{3u} = upper bound wave numbers
M = Mach number, U_∞/a_∞
m, n = mode numbers
$\bar{p}$ = $a^2b^2p(\bar{x}, \bar{y}, \bar{t})/hD$
$p(\bar{x}, \bar{y}, \bar{t})$ = turbulent pressure, three-dimensional homogeneous Gaussian process
$\bar{p}^e$ = $a^2b^2p^e(\bar{x}, \bar{y}, \bar{t})/hD$
$p^e(\bar{x}, \bar{y}, \bar{t})$ = fluid pressure, external flow
$\bar{p}^c$ = $a^2b^2p^c(\bar{x}, \bar{y}, \bar{t})/hD$
$p^c(\bar{x}, \bar{y}, \bar{t})$ = fluid pressure, cavity flow
R = spatial region of integration
q = $\rho_\infty U_\infty{}^2/2$, dynamic pressure
t = time
$\bar{t}$ = $t(D/\rho)^{1/2}/ab$
T = triangular matrix
t_{ij} = elements of matrix **T**
U_c = convectional speed
U_∞ = mean external flow velocity
w = plate deflection
$\bar{w}$ = w/h
x, y, z = spatial coordinates
x_1, x_2, x_3 = spatial coordinates
$\bar{x}$ = x/a
x = x_1, x_2, x_3
$\bar{y}$ = y/b
$\bar{z}$ = z/d
α = a/b
β_1, β_2 = damping coefficients
$\bar{\nabla}^2$ = $[(b/a)\partial^2/\partial\bar{x}^2 + (a/b)\partial^2/\partial\bar{y}^2]$
ζ = boundary-layer displacement thickness
ζ^* = boundary-layer thickness
λ = $2qab^2/D$
λ^c = $\rho_c a_c{}^2 ab^2/D$
ν = Poisson's ratio
ρ = plate density/unit area
ρ_∞ = freestream density
ρ_c = cavity flow density
σ_p = root mean square pressure of boundary-layer pressure fluctuations
$\sigma_{\bar{p}}$ = $a^2b^2\sigma_p/hD$
$\bar{\phi}$ = airy stress function for membrane stresses
ϕ, ϕ^c = velocity potential, external and cavity flows
ω = frequency
ω_l, ω_u = lower bound and upper bound frequencies, respectively

Received July 7, 1971; revision received February 14, 1972. This work reported herein was supported by NSF Grant GK 3858 and GK 24925.

Index categories: Structural Dynamic Analysis; Aeroelasticity and Hydroelasticity.

* Assistant Professor of Civil Engineering and Engineering Mechanics. Associate Member AIAA.

† Research Assistant.

‡ Professor of Civil Engineering and Engineering Mechanics. Member AIAA.

1. Introduction

PROBLEMS associated with noise estimation and structural fatigue are of considerable importance from an environmental and structural integrity point of view. It is well established by now that the surface of a vehicle traveling at high speed through air can be severely excited by a turbulent boundary layer which envelops the external surface of the vehicle. The turbulent boundary-layer induced vibrations could inflict fatigue damage on the structure. Such fatigue stresses must be taken into consideration in designing these vehicles to have a considerable service life. However, to assess the fatigue life of the vibrating structure, it is necessary to know the structural response.

The random vibration of a flexible plate immersed in a fluid flow on one side and backed by a fluid filled cavity of finite dimensions on the other side is considered in this analysis (Fig. 1). The nonlinear plate stiffness induced in the plate by out-of-plane

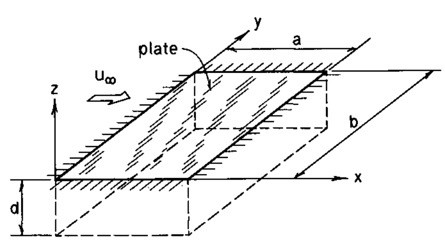

Fig. 1 Problem geometry.

bending and the mutual interaction between the external and internal fluid flow is included. A similar problem was considered by Dowell[6] where the boundary-layer pressure field was idealized as Gaussian white noise. No such assumption is made in this paper.

A Monte Carlo technique is utilized for the response analysis of the plate undergoing large deformations under the turbulent boundary-layer pressure excitation. The pressure field acting on the plate is decomposed into three parts: the external flow (radiation) pressure, the internal (cavity) pressure, and the random pressure resulting from the boundary-layer pressure fluctuations. The random pressure field is taken as a stationary and homogeneous multidimensional Gaussian process having a mean value equal to zero.

The analysis is performed in time domain rather than in frequency or wave number domain as usually done in linear response analysis. This is achieved by simulating the generalized forces in time domain. The simulation technique developed by Shinozuka[10,11] is a major breakthrough in the time-domain approach since this enables us to include in dynamic analysis multidimensional or multivariate Gaussian processes which have specified cross spectral densities. The essential features of this approach is that a random process can be simulated by a series of cosine functions with weighted amplitudes, almost evenly spaced random frequencies (or wave numbers), and random phase angles which are uniformly distributed between 0 and 2π. Thus, the method does not require filtering a random process.

Numerical examples are presented for subsonic and supersonic flow regions. In both cases it is assumed that the vibrating panel does not affect the structure of the boundary-layer turbulence. It is shown that for supersonic flow a panel flutter region can be obtained by simply increasing dynamic pressure until a limit cycle amplitude is reached.

2. Panel Response

The deflection w of a simply supported panel immersed in a fluid flow and having a geometric nonlinearity can be described by two partial differential equations which are given in Refs. 1 and 6.

In solving these equations, the plate deflection $\bar{w}$ is expanded in terms of normal modes of the corresponding linear plate

$$\bar{w}(\bar{x},\bar{y},\bar{t}) = \sum_{m=1}\sum_{n=1} b_{mn}(\bar{t})\sin m\pi\bar{x}\sin n\pi\bar{y} \tag{1}$$

After the required stress function is evaluated, the assumed modal solution is satisfied in Galerkin sense by computing its integral average weighted in turn by each term of Eq. 1. The result is a system of simultaneous nonlinear integral-differential equations for $b_{mn}(\bar{t})$ which involve the generalized forces

$$\bar{F}_{mn}(\bar{t}) = (a^2b^2/hD)\int_0^1\int_0^1 p(\bar{x},\bar{y},\bar{t})\sin m\pi\bar{x}\sin n\pi\bar{y}\,d\bar{x}\,d\bar{y} \tag{2a}$$

$$\bar{F}_{mn}{}^{e}(\bar{t}) = (a/h\rho_\infty U_\infty{}^2)\int_0^1\int_0^1 p^e(\bar{x},\bar{y},\bar{t})\sin m\pi\bar{x}\sin n\pi\bar{y}\,d\bar{x}\,d\bar{y} \tag{2b}$$

$$\bar{F}_{mn}{}^{c}(\bar{t}) = (a/h\rho_c a_c{}^2)\int_0^1\int_0^1 p^c(\bar{x},\bar{y},\bar{t})\sin m\pi\bar{x}\sin n\pi\bar{y}\,d\bar{x}\,d\bar{y} \tag{2c}$$

where p^e and p^c are the external and cavity pressures, respectively, due to the plate motion.

To promote computation ease and to demonstrate the applications of the general method, a two mode approximation is assumed to Eq. (1) corresponding to x coordinate and one mode approximation corresponding to y coordinate. Then the solution for the stress function $\bar{\phi}$ with the "average in plane boundary conditions of $\bar{\phi}$"[1]

$$\int_0^a\int_0^b \partial u/\partial x\,dx\,dy = 0;\quad \int_0^a\int_0^b \partial v/\partial y\,dx\,dy = 0 \tag{3}$$

is given by

$$\begin{aligned}\bar{\phi} = {}& [\pi^2Eh^3/16D(1-\nu^2)\alpha^2]\{[(1+\nu\alpha^2)b_1{}^2+(4+\nu\alpha^2)b_2{}^2]\bar{y}^2+\\ & [(\alpha^2+\nu)b_1{}^2+(\alpha^2+4\nu)b_2{}^2]\alpha^2\bar{x}^2\}+(Eh^3\alpha^2/4D)\times\\ & \{[(b_1{}^2/8)\cos 2\pi\bar{x}-b_1b_2\cos\pi\bar{x}+(b_1b_2/9)\cos 3\pi\bar{x}+\\ & (b_2{}^2/32)\cos 4\pi\bar{x}]+[(b_1{}^2+4b_2{}^2)/8\alpha^4+\\ & [9b_1b_2/(1+4\alpha^2)^2]\cos\pi\bar{x}-[b_1b_2/(9+4\alpha^2)^2]\times\\ & \cos 3\pi\bar{x}\cos 2\pi\bar{y}\}\end{aligned} \tag{4}$$

where u and v are in-plane displacements and the second subscript on the generalized coordinate has been omitted for simplicity. Substituting Eq. (1) into given governing equations and employing Eq. (4) yields

$$\ddot{b}_1+\beta_1\dot{b}_1+(C_{10}+C_{11}b_1{}^2+C_{12}b_2{}^2)b_1 = 4(\bar{F}_1+\lambda\bar{F}_1{}^e+\lambda^c\bar{F}_1{}^c) \tag{5a}$$

$$\ddot{b}_2+\beta_2\dot{b}_2+(C_{20}+C_{21}b_1{}^2+C_{22}b_2{}^2)b_2 = 4(\bar{F}_2+\lambda\bar{F}_2{}^e+\lambda^c\bar{F}_2{}^c) \tag{5b}$$

where

$$C_{10} = (\alpha+1/\alpha)^2\pi^4;\quad C_{20} = (\alpha+4/\alpha)^2\pi^4;$$

$$C_{11} = (\tfrac{3}{4})\pi^4[(1-\nu^2)(\alpha^2+1/\alpha^2)+2(2\nu+\alpha^2+1/\alpha^2)];$$

$$C_{12} = (\tfrac{3}{4})\pi^4\{(1-\nu^2)[4(\alpha^2+1/\alpha^2)+81\alpha^2/(1+4\alpha^2)^2+\alpha^2/(9+4\alpha^2)^2]+2(5\nu+\alpha^2+4/\alpha^2)\};$$

$$C_{21} = C_{12};$$

$$C_{22} = (\tfrac{3}{4})\pi^4[(1-\nu^2)(\alpha^2+16/\alpha^2)+2(8\nu+\alpha^2+16/\alpha^2)]$$

Then b_1 and b_2 are obtained by solving Eqs. (5a) and (5b) simultaneously by Monte Carlo technique.

3. Simulation of a Multidimensional Random Process

Consider a homogeneous random process, $f(t,\mathbf{x})$, with mean zero and spectral density function $S(\omega, k_1, k_2, k_3)$ specified in the region

$$-\infty < (\omega_l, k_{1l}, k_{2l}, k_{3l}) \leqq (\omega, k_1, k_2, k_3) \leqq (\omega_u, k_{1u}, k_{2u}, k_{3u}) < \infty$$

where ω is frequency and k_i are wave numbers in x_i ($i = 1, 2, 3$) directions, respectively. Denote the interval by

$$(\Delta\omega, \Delta k_1, \Delta k_2, \Delta k_3) = [(\omega_u-\omega_l)/N_1,\quad (k_{1u}-k_{1l})/N_2,\quad (k_{2u}-k_{2l})/N_3,\quad (k_{3u}-k_{3l})/N_4]$$

Then, the random process $f(t,\mathbf{x})$ can be simulated by the following series

$$f(t,\mathbf{x}) = (2)^{1/2}\sum_{i=1}^{N_1}\sum_{j=1}^{N_2}\sum_{r=1}^{N_3}\sum_{n=1}^{N_4} A_{ijrn}\cos(\omega_i't+k_{1j}'x_1+k_{2r}'x_2+k_{3n}'x_3+\phi_{ijrn}) \tag{6}$$

where

$$A_{ijrn} = [S(\omega_i, k_{1j}, k_{2r}, k_{3n})\Delta\omega\Delta k_1\Delta k_2\Delta k_3]^{1/2}$$

ϕ_{ijrn} = independent random phase angles uniformly distributed between 0 and 2π.

$$(\omega_i', k_{1j}', k_{2r}', k_{3n}') = (\omega_i+\delta\omega, k_{1j}+\delta k_1, k_{2r}+\delta k_2, k_{3n}+\delta k_3)$$

$$(\omega_i, k_{1j}, k_{2r}, k_{3n}) = [\omega_l+(i-\tfrac{1}{2})\Delta\omega,\ k_{1l}(j-\tfrac{1}{2})\Delta k_1,\ k_{2l}+(r-\tfrac{1}{2})\Delta k_2,\ k_{3l}+(n-\tfrac{1}{2})\Delta k_3]$$

in which $(\delta\omega, \delta k_1, \delta k_2, \delta k_3)$ are small random frequencies (or wave numbers) introduced to avoid the periodicity of the simulated process, and are uniformly distributed between

$$(-\Delta\omega'/2, -\Delta k_1'/2, -\Delta k_2'/2, -\Delta k_3'/2)$$

and

$$(\Delta\omega'/2, \Delta k_1'/2, \Delta k_2'/2, \Delta k_3'/2)$$

with

$$(\Delta\omega', \Delta k_1', \Delta k_2', \Delta k_3') \ll (\Delta\omega, \Delta k_1, \Delta k_2, \Delta k_3)$$

When performing modal analysis in a Galerkin sense, it is advantageous to simulate the resulting generalized random forces.

Considering the random excitation field to be $f(t, \mathbf{x})$, the generalized force $F_m(t)$ corresponding to the mth mode $\xi_m(\mathbf{x})$ can be written as

$$F_m(t) = \int_R f(t, \mathbf{x}) \xi_m(\mathbf{x})\, d\mathbf{x} \tag{7}$$

Utilizing Eqs. (6) and (7), the generalized random force takes the form

$$F_m(t) = (2)^{1/2} \sum_{i=1}^{N_1} (G_{mi} \cos \omega_i' t - H_{mi} \sin \omega_i' t) \tag{8}$$

where

$$G_{mi} = \sum_{j=1}^{N_2} \sum_{r=1}^{N_3} \sum_{n=1}^{N_4} A_{ijrn}(B_{mjrn} \cos \phi_{ijrn} - D_{mjrn} \sin \phi_{ijrn}) \tag{9a}$$

$$H_{mi} = \sum_{j=1}^{N_2} \sum_{r=1}^{N_3} \sum_{n=1}^{N_4} A_{ijrn}(B_{mjrn} \sin \phi_{ijrn} + D_{mjrn} \cos \phi_{jirn}) \tag{9b}$$

and

$$B_{mjrn} = \int_R \cos(k_{1j}' x_1 + k_{2r}' x_2 + k_{3n}' x_3) \xi_m(\mathbf{x})\, d\mathbf{x} \tag{10a}$$

$$D_{mjrn} = \int_R \sin(k_{1j}' x_1 + k_{2r}' x_2 + k_{3n}' x_3) \xi_m(\mathbf{x})\, d\mathbf{x} \tag{10b}$$

It is important to note that the integration given in Eqs. (10a) and (10b) can be usually carried out in a closed form. Furthermore, G_{mi} and H_{mi} are independent of time and need to be computed only once. Therefore, the number of terms in the series is reduced from $N_1 \times N_2 \times N_3 \times N_4$ to N_1 for the subsequent numerical integration in time domain.

It can be shown that the generalized force simulated by Eq. (8) is ergodic only as $N_1 \to \infty$. Since ergodicity is important in time domain analysis, it is advantageous to modify the simulation technique so that the simulated generalized force is ergodic for any finite number of N_1.

Consider M generalized forces corresponding to M modes as expressed in Eq. (8). Then it can be shown that the cross spectral density function can be written as

$$S_{mp}(\omega_i) = (1/\Delta\omega)(C_{mpi} - \mathbf{i} Q_{mpi}) \qquad i = 1, 2, \ldots N_1 \tag{11}$$

where

$$C_{mpi} = \sum_{j=1}^{N_2} \sum_{r=1}^{N_3} \sum_{n=1}^{N_4} A_{ijrn}^2 (B_{mjrn} B_{pjrn} + D_{mjrn} D_{pjrn})$$

$$Q_{mpi} = \sum_{j=1}^{N_2} \sum_{r=1}^{N_3} \sum_{n=1}^{N_4} A_{ijrn}^2 (B_{mjrn} D_{pjrn} - B_{pjrn} D_{mjrn})$$

The cross spectral density matrix $\mathbf{S}$ corresponding to Eq. (11) can be decomposed into a lower triangular matrix $\mathbf{T}$ such that

$$\mathbf{S} = \mathbf{T}(\mathbf{T}^*)' \tag{12}$$

where a star indicates matrix conjugation and a prime indicates matrix transposition. Then, the generalized random force is simulated by

$$F_m(t) = (2)^{1/2} \sum_{s=1}^{m} \sum_{i=1}^{N_1} |t_{ms}(\omega_i)| (\Delta\omega)^{1/2} \times \cos(\omega_i' t + \theta_{ms}(\omega_i) + \phi_{si}) \tag{13}$$

where

$$\theta_{ms}(\omega_i) = \tan^{-1}\{[\operatorname{Im} t_{ms}(\omega_i)]/\operatorname{Re} t_{ms}(\omega_i)\}$$

ϕ_{si} = independent random phase angles uniformly distributed between 0 and 2π. For more detailed treatment on the simulation of random processes see Refs. 10 and 11.

4. External and Internal Flow Solutions

By assuming the external flow to be inviscid and irrotational, the pressure on the plate can be determined from potential flow equations given in Ref. 6. These equations can be solved by employing Laplace transform with respect to time and Fourier transform with respect to space domain. This method has been used in Ref. 5. Without repeating the lengthy but straightforward calculations, we express the generalized aerodynamic force of the external flow as

$$\bar{F}_m^{\,e} = \sum_r Q_{rm} \tag{14}$$

where Q_{rm} is given in Refs. 5 and 6. For high Mach numbers, Eq. (14) can be approximated to

$$\bar{F}_m^{\,e}(\bar{t}) = \sum_{r=1} [E_{rm} b_r(\bar{t}) + P_{rm} \dot{b}_r(\bar{t})] \tag{15}$$

where

$$\begin{aligned} E_{rm} &= rm[1-(-1)^{r+m}]/[2M(m^2-r^2)] && \text{for } r \neq m \\ &= 0 && \text{for } r = m \\ P_{rm} &= (D/\rho)^{1/2}/4MbU_\infty && \text{for } r = m \\ &= 0 && \text{for } r \neq m \end{aligned}$$

The fluid motion in the cavity may be described by the velocity potential ϕ^c satisfying the wave equation.[6] By taking Fourier transform with respect to time, this equation reduces to Helmholtz equation which can be solved by relating the velocity potential to the panel displacement field through use of Green's Theorem. However, for a shallow cavity, $a/d \gg 1$ (Ref. 6), the generalized cavity force can be expressed as

$$\bar{F}_m^{\,c} = -a[1-(-1)^m] \sum_{r=1} [1-(-1)^r] b_r/(\pi^4 dmr) \tag{16}$$

Employing the shallow cavity approximation, the pressure inside the cavity is obtained from

$$p^c = -2p_c a_c^2 h \sum_{r=1} [1-(-1)^r] b_r/(\pi^2 dr) \tag{17}$$

which implies that for this case the pressure is spatially constant throughout the cavity. As pointed out in Ref. 6 and also observed in this analysis, Eqs. (16) and (17) are useful approximations when calculating the plate response and pressure inside a shallow cavity. However, the noise levels produced inside the cavity need to be obtained utilizing the more general expressions given in Ref. 6.

5. Numerical Examples

The numerical examples were worked out on an IBM 360/91. The following physical data were used in the computation: $a = 10$ in.; $b = 20$ in.; $d = 5$ in.; $\nu = 0.3$; $\rho = 0.1 \times h$ lb/in.^{2}; $E = 10^7$ psi. The thickness of the plate was varied in such a way that either the nondimensional turbulent pressure $\bar{p}$ or the dynamic pressure parameter λ was adjusted for the convenience of illustration. The damping coefficients β_1 and β_2 were taken as 1% of critical damping of the 1st and 2nd modes of the linear plate, respectively. The generalized forces were simulated using $N_1 = 100$, $N_2 = 40$, $N_3 = 40$. The shallow cavity approximation corresponding to Eq. (16) was used for all examples.

Subsonic Flow

For this case, the semiempirical formula of cross spectral density corresponding to subsonic boundary-layer turbulence obtained in Ref. 3 is used

$$\begin{aligned} S(\omega, k_1, k_2) = {} & 0.715 \times 10^{-6} (q^2 \zeta/\pi^2 U_\infty)[3.7 \exp(-2|\omega|\zeta/U_\infty) + \\ & 0.8 \exp(-0.47|\omega|\zeta/U_\infty) - 3.4 \exp(-8|\omega|\zeta/U_\infty)] \cdot \\ & (\omega/U_c)^2/[(0.1\omega/U_c)^2 + (|\omega|/U_c + k_1)^2][(0.715\omega/U_c)^2 + k_2^2] \end{aligned} \tag{18}$$

where $U_c = 0.65 U_\infty$ and the rms of the pressure in Eq. (18) was taken as $\sigma_p = 0.0056q$. Assuming an altitude of 30,000 ft and no static pressure differential across the plate, $\rho_\infty = \rho_c = 0.00089$ slugs/ft^3 and $a_\infty = a_c = 995$ fps. Corresponding to the freestream velocity of $U_\infty = 800$ fps, the displacement thickness was taken as $\zeta = 0.157$ in. The effect of the external fluid pressure on the

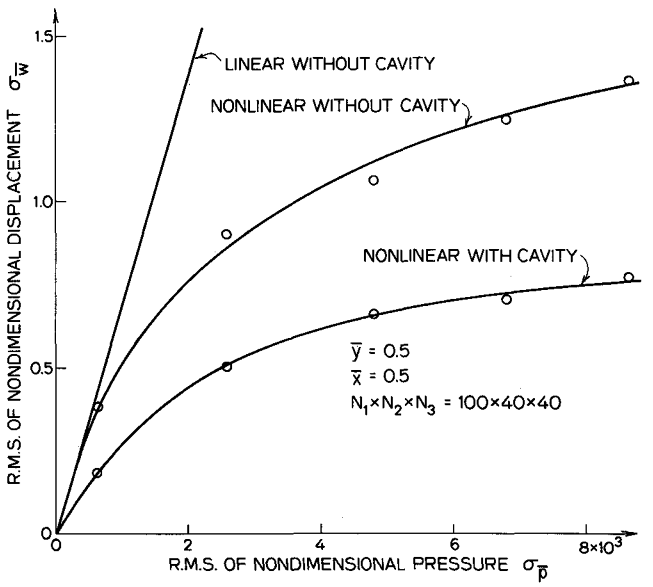

Fig. 2 The rms response of the plate.

plate response due to the plate motion was neglected in this example.

The nondimensional rms response at the center of the plate vs the nondimensional rms pressure (with the plate thickness ranging from 0.015 in. to 0.03 in.) is plotted in Fig. 2 with and without the cavity effect. For the purpose of comparison, the response corresponding to a linear plate is also presented in Fig. 2. In Fig. 3, a portion of the time history of the nondimensional response at $\bar{x} = 0.75, \bar{y} = 0.5$ is plotted for $\sigma_{\bar{p}} = 7500$. The response is a narrow band random process with the apparent frequency varying as shown in Fig. 4. Similar result was obtained for a deterministic case.[4]

Supersonic Flow

Following the measurements and observations made by Maestrello,[9] the spectral density function corresponding to a supersonic boundary-layer turbulence is taken as

$$S(\omega, k_1, k_2) = \sigma_p{}^2(\zeta^*/\pi^2 U_\infty)[0.044\exp(-0.0578\,|\omega|\,\zeta^*/U_\infty) + 0.075\exp(-0.243\,|\omega|\,\zeta^*/U_\infty) - 0.093\exp(-1.12\,|\omega|\,\zeta^*/U_\infty) - 0.025\exp(-11.57\,|\omega|\,\zeta^*/U_\infty)]\,1/\alpha_1\,\alpha_2\,\zeta^*\zeta^*[(1/\alpha_1\,\zeta^*)^2 + (|\omega|/U_c + k_1)^2][(1/\alpha_2\,\zeta^*)^2 + k_2{}^2] \quad (19)$$

where $U_c = 0.75 U_\infty$, $\sigma_p = 0.005q$, $\alpha_2 = 0.26$. For $M = 2$ and $U_\infty = 1942$ fps at 45,000 ft altitude: $\rho_\infty = \rho_c = 0.0004605$ slug/ft^3, $a_\infty = a_c = 971$ fps, $\zeta^* = 0.91$, $\alpha_1 = 1.22$. To reduce computation time, the generalized aerodynamic force given in Eq. (15) was used.

The nondimensional amplitudes of the plate response at $\bar{y} = 0.5, \bar{x} = 0.75$ are plotted against the dynamic pressure parameter λ in Fig. 5 for the plate with and without the cavity effect. In Fig. 7, portions of the time history of the plate response for several values of λ are shown. For λ equal or larger than 1900, a sinusoidal type oscillation (known as limit cycle oscillation) is reached. As it is evident from Fig. 7, the boundary-layer turbulence corresponding to $\sigma_p = 0.005q$ has no significant effect on the plate response near and inside the flutter region. However, by increasing turbulent energy to $\sigma_p = 0.025q$, the plate response is modified significantly by the turbulent pressure fluctuations as shown in Fig. 8. The streamwise panel deflection shapes are plotted in Fig. 6 with the maximum deflection occurring roughly at $\bar{x} = 0.75, \bar{y} = 0.5$.

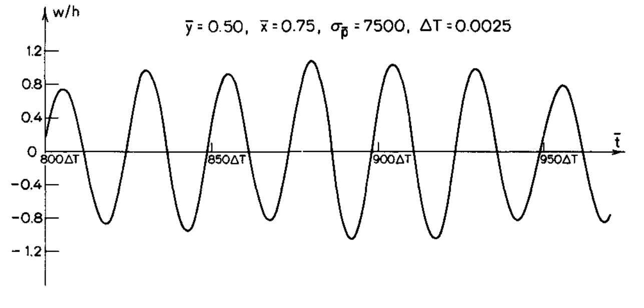

Fig. 3 Time history of plate response (with cavity).

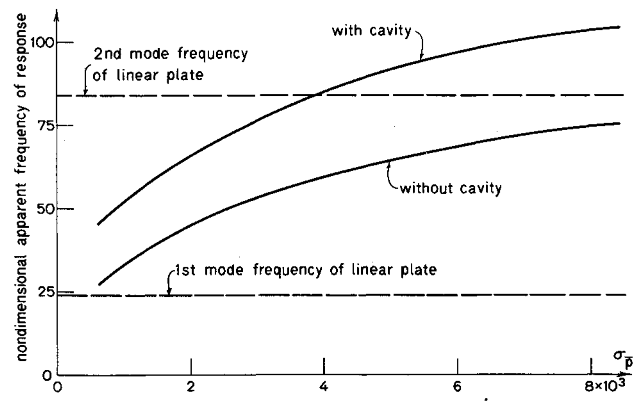

Fig. 4 Apparent frequency of response.

6. Discussion and Conclusions

The method considered in this paper provides an efficient tool in dealing with nonlinear response of panels exposed to subsonic and supersonic boundary-layer turbulence. It is not limited to only low-intensity excitations such as the case for perturbation, linearization and other standard techniques used for nonlinear problems. The approach may be used to study panel response and noise transmission to any external force, not only boundary-layer pressure. The "noise" and "flutter" problems are treated in the same unified manner. Flutter condition is simply obtained from the response of the plate exhibiting a sustained cycle oscillation.

The effect of cavity on panel response was analyzed on the basis that the cavity acts as an air-spring resisting the modes that tend to compress the air raising their modal frequencies. Since only odd modes involve compression, the air spring effect

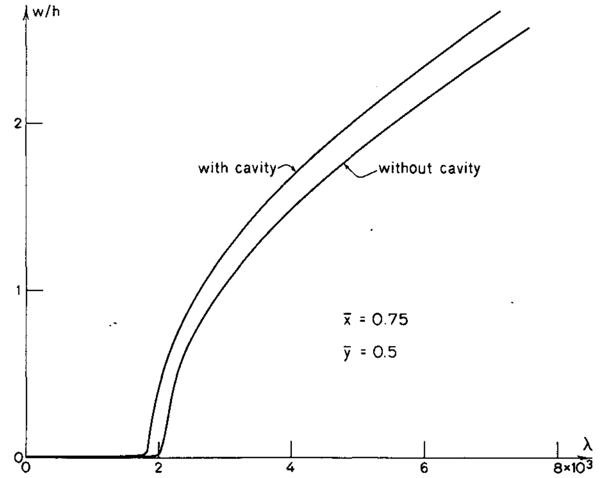

Fig. 5 Limit cycle amplitude vs dynamic pressure parameter λ.

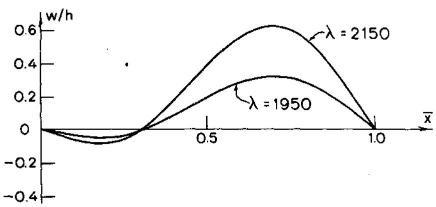

Fig. 6 Deflection shape of flutter motion.

is the largest on the first mode. Thus for subsonic case the response is reduced substantially by the presence of a cavity. However, for supersonic flow flutter occurred at a lower dynamic pressure with cavity than for the case without cavity. This was due to the fact that the first mode frequency was raised by the aerodynamic spring effect producing an earlier coupling between the first and second mode frequencies, thereby inducing flutter. Furthermore, it was found that for supersonic flow the pressure induced by the panel motion cannot be neglected. The total damping in the system is dominated by the aerodynamic damping which is associated with the energy radiating field.

The boundary-layer turbulence, in general, is a broad band random process. This suggests that many modes could be excited with the strongest excitation occurring when the pressure wave of the boundary-layer turbulence and the flexure wave of the panel match in both speed and wave number. The previous investigations on panel flutter indicate that at least four streamwise modes need to be taken to obtain results of reasonable accuracy. Furthermore, the analysis on noise transmission might require to include even higher modes since for some cases the main contribution to the noise energy comes from frequencies associated with high modes. The present method is not limited to any number of modes and only to save computation time a two mode approximation has been used for the illustrative examples.

The rms responses were obtained by taking the temporal average over the time interval of 100 fundamental periods of the corresponding linear plate. The time required to simulate a point (open circle in Fig. 4) is of the order of 100 sec on IBM 360/91 computer. Thus, the curves given in Fig. 4 were produced in approximately 17 min. When higher plate modes are considered,

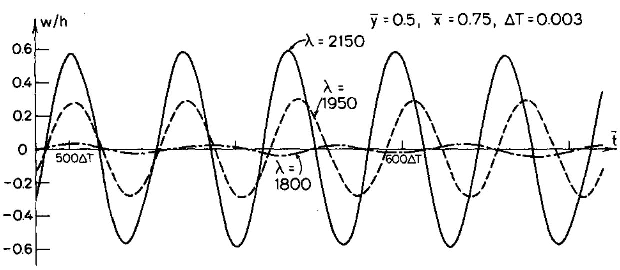

Fig. 7 Time history of response with $\sigma_p = 0.005q$.

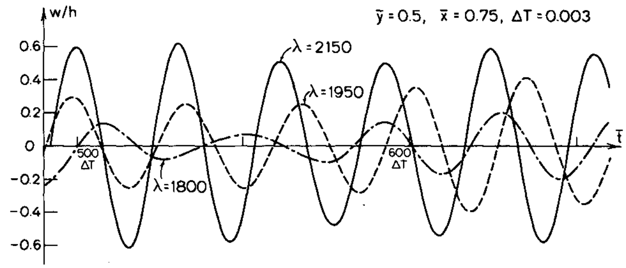

Fig. 8. Time history of response with $\sigma_p = 0.025q$.

it is necessary to increase the cut-off bounds on the frequency and wave number spectrum in order to include in the simulation process frequencies or wave numbers associated with these higher modes. This increases computation time, mainly not for simulation process, but for numerical integration of simultaneous nonlinear differential equations.

References

[1] Bolotin, V. V., *Nonconservative Problems of the Theory of Elastic Stability*, Pergamon Press, New York, 1963, pp. 280–289.

[2] Bull, M. K., Wilby, J. F., and Blackman, D. R., "Wall Pressure Fluctuation in Boundary Layer Flow and Response of Simple Structure to Random Pressure Fields," A.A.S.U. Rept. 243, 1963, Univ. of Southampton, Southampton, England, pp. 1–28.

[3] Bull, M. K., "Wall-Pressure Fluctuation Associated with Subsonic Turbulent Boundary Layer Flow," *Journal of Fluid Mechanics*, Vol. 28, Pt. 4, 1967, pp. 719–754.

[4] Chu, M. and Herrmann, G., "Influence of Large Amplitude on Free Flexural Vibration of Rectangular Elastic Plates," *Journal of Applied Mechanics*, Vol. 23, No. 4, Dec. 1956, pp. 532–540.

[5] Dowell, E. H., "Generalized Aerodynamic Forces on a Flexible Plate Undergoing Transient Motion," *Quarterly of Applied Mathematics*, Vol. 24, 1967, pp. 331–338.

[6] Dowell, E. H., "Transmission of Noise from a Turbulent Boundary Layer through a Flexible Plate into a Closed Cavity," *Journal of Acoustical Society of America*, Vol. 46, No. 1, Pt. 2, 1969, pp. 238–252.

[7] Dowell, E. H., "Panel Flutter: A Review of Aeroelastic Stability of Plates and Shells," *AIAA Journal*, Vol. 8, No. 3, March 1970, pp. 385–399.

[8] Maestrello, L., "Measurement and Analysis of the Response Field of Turbulent Boundary Layer Excited Panels," *Journal of Sound and Vibration*, Vol. 2, 1965, pp. 270–292.

[9] Maestrello, L., "Radiation from a Panel Response to a Supersonic Turbulent Boundary Layer," *Journal of Sound and Vibration*, Vol. 10, pp. 261–295.

10 Shinozuka, M., "Simulation of Multivariate and Multidimensional Random Processes," *Journal of Acoustical Society of America*, Vol. 49, No. 1, Pt. 2, 1971, pp. 357–367.

[11] Shinozuka, M. and Jan, C.-M., "Simulation of Multivariate and Multidimensional Random Processes II," NSF GK-3858 and GK-24925, TR 12, 1971, Columbia University, New York.

[12] Shinozuka, M. and Wen, Y.-K., "Monte Carlo Solution of Nonlinear Vibrations," *AIAA Journal*, Vol. 10, No. 1, Jan. 1972, pp. 37–40.